

Using the GOES-16 Split Window Difference to Detect a Boundary prior to Cloud Formation

DANIEL T. LINDSEY, DAN BIKOS, AND LEWIS GRASSO

BACKGROUND. The Geostationary Operational Environmental Satellite R series (GOES-R) was launched in November 2016, and upon reaching geostationary orbit a few weeks later it became *GOES-16* (Schmit et al. 2017) and was placed at 89.5°W longitude for checkout. Its Advanced Baseline Imager (ABI) provides improved spectral, spatial, and temporal resolution compared to the previous GOES imagers, allowing forecasters to detect some meteorological phenomena that were previously not possible. In preparation for the data the ABI would be sending back, studies were performed over the last 10 years using proxy ABI data. One such study by Lindsey et al. (2014) used output from the 4-km National Severe Storms Laboratory (NSSL) Advanced Research version of the Weather Research and Forecasting (WRF-ARW) Model and a radiative transfer model to simulate the ABI's 10.3- and 12.3- μm bands to analyze the low-level pooling of water vapor. They showed that in clear sky conditions and when the temperature decreases with height in the low levels (which is frequently the case following the mix-out of any low-level temperature inversion), regions with locally deeper water vapor will be associated with local maxima in the difference between 10.3 and 12.3 μm , referred to as the split window difference (SWD). This idea goes back to work by Chesters et al. (1983), but only recently have satellites in geostationary orbit

had the necessary pixel spacing and other important attributes to detect small-scale gradients in the SWD, like those that may occur along a surface boundary. *GOES-16* ABI's infrared bands have 2-km pixel spacing at nadir and the continental United States is scanned every 5 min.

In the absence of clouds, radiation emitted by the surface at 10.3 μm makes it to the satellite without significant absorption by atmospheric water vapor (Lindsey et al. 2012); for this reason it is referred to as a “clear window” band. Radiation at 12.3 μm coming from the surface is preferentially absorbed by water vapor (compared to 10.3 μm), resulting in its nickname of the “dirty window.” When the temperature decreases with height above the surface, the water vapor absorbs and reemits the radiation at a cooler temperature, and this effect is greater with the 12.3- μm band compared to the 10.3- μm band, meaning the brightness temperature detected by the satellite will be warmer at 10.3 than at 12.3 μm . As the depth of water vapor increases into regions of colder temperatures, the SWD will increase. Figure 2 in Lindsey et al. (2014) quantifies these changes using a series of idealized atmospheric profiles of temperature and water vapor. Now that the *GOES-16* ABI is sending back data, case studies have been collected using *observed* data, as opposed to *simulated* satellite imagery. The case presented here is from 15 June 2017 over western and central Kansas. Note that the satellite data used in this analysis were still preliminary and nonoperational.

AFFILIATIONS: LINDSEY—National Oceanic and Atmospheric Administration/Center for Satellite Applications and Research, Fort Collins, Colorado; BIKOS AND GRASSO—Cooperative Institute for Research in the Atmosphere, Fort Collins, Colorado

CORRESPONDING AUTHOR: Daniel T. Lindsey, dan.lindsey@noaa.gov

DOI:10.1175/BAMS-D-17-0141.1

A supplement to this article is available online (10.1175/BAMS-D-17-0141.2).

©2018 American Meteorological Society

For information regarding reuse of this content and general copyright information, consult the [AMS Copyright Policy](#).

CONDITIONS ON 15 JUNE 2017. On 15 June 2017, the National Weather Service's Storm Prediction Center issued an “enhanced risk” of severe storms across portions of central and southeast Kansas. Figure 1 shows band-2 visible satellite imagery and surface observations from that morning at 1302 UTC. Skies were almost completely clear, while temperatures and dewpoints were higher in the southern half of the state compared to the northern portion.

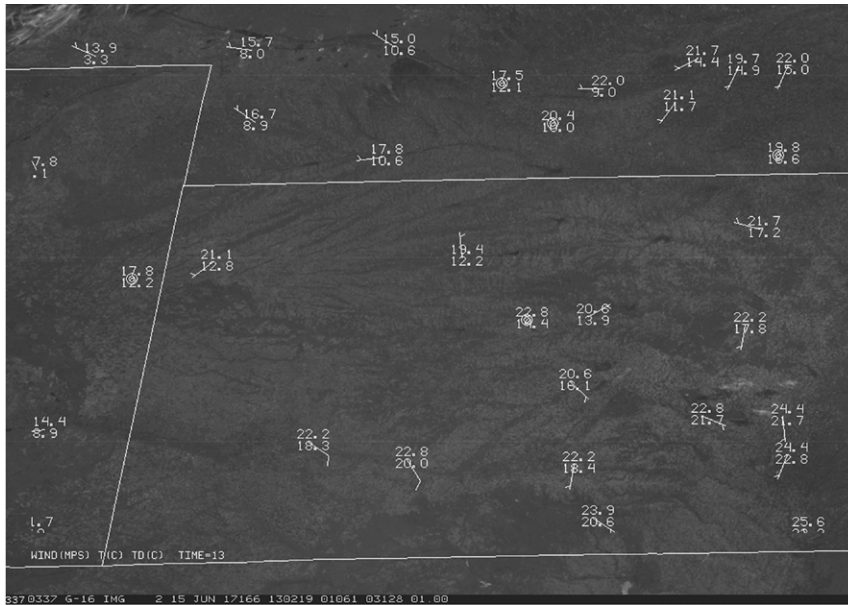


FIG. 1. GOES-16 0.64- μm visible satellite image at 1302 UTC 15 Jun 2017, and surface observations showing (top) temperature and (bottom) dewpoint temperature in $^{\circ}\text{C}$ and wind barbs where a full barb represents 10 m s^{-1} .

Observed wind directions along with the surface observations suggested the presence of a low-level convergence boundary stretching roughly east–west across western Kansas given the southeasterly winds in southwest Kansas and weak northerly or northwesterly winds in northern Kansas and portions of southern Nebraska. Determining the specific location of the boundary is difficult for forecasters because the density of surface observations across western Kansas is relatively low. The lack of clouds in the visible channel also makes the location determination difficult based on traditional satellite cues. Boundaries are important because they often serve as the focal point for convective cloud and sometimes storm formation later in the day (e.g., Purdom 1976).

Figure 2 shows several forecast fields from the 1200 UTC cycle of the Global Forecast System (GFS) model valid at 1500 and 1800 UTC. The plan views (Figs. 2a,b) show dewpoints were around 70°F in south-central Kansas (red colors), with the pool of moist air at the surface extending into western Kansas. The location of the boundary can best be seen in the model field by looking at the wind barbs. The 3-h forecast valid at 1500 UTC shows an east–west boundary in extreme northwestern Kansas (Fig. 2a, white dashed line); then by 1800 UTC the portion of the boundary in western Kansas is farther south and connected to a local cyclonic circulation in west-central Kansas, while the

eastern part of the boundary has moved northward into northern Kansas and is oriented southwest to northeast (Fig. 2b, white dashed line). A forecaster in this situation would be looking for observations to check the accuracy of the model’s placement of the surface boundary.

Convective evolution is dependent not only on surface conditions but also on above-the-surface profiles of temperature and water vapor, particularly in the boundary layer. Figures 2c and 2d show north–south vertical cross sections across the cyan line in Figs. 2a and 2b, respectively, from the same GFS forecast. The location of the surface boundary

can be seen in Fig. 2c by examining the lowest wind vectors; the wind direction shifts from southerly to south–southwesterly near the yellow line marked B. At 1800 UTC (Fig. 2d) the model shifts the surface boundary southward toward a local maximum in low-level water vapor (yellow line marked B in Fig. 2d), and the depth of low-level water vapor increases slightly between 1500 and 1800 UTC at levels below 700 hPa; this can be seen by noting the 12 g kg^{-1} mixing ratio contour rising between Figs. 2c and 2d. The slight deepening of water vapor may be forced by low-level convergence of water vapor along the surface boundary in the model.

USING THE SPLIT WINDOW DIFFERENCE TO LOCATE THE SURFACE BOUNDARY.

Animation 1 (animations can be viewed in the online supplement; <https://doi.org/10.1175/BAMS-D-17-0141.2>) provides a time series of the GOES-16 0.64- μm band-2 visible imagery from 1302 to 1957 UTC, and animation 2 is the corresponding GOES-16 10.3–12.3- μm SWD from 1322 to 1957 UTC with surface observations overlaid (see Fig. 3 for the SWD legend). Figure 3 provides two select times from those animations spaced 4 h apart beginning at 1502 UTC. The SWD legend is designed such that colors from green to yellow to orange to red correspond to increasingly positive values. From 1302 through 1542 UTC, the

0.64 μm visible image in animation 1 shows completely clear skies in western Kansas. At those same times, a local linear maximum in SWD becomes evident in western Kansas, shifting southward with time. Values of SWD increase with time throughout the animation owing to surface heating, but the local linear maximum is easy to pinpoint amid the more widespread increases (see the black arrows in Fig. 3b). This local maximum is very likely collocated with the surface boundary as suggested by the GFS model forecast, except the location of the boundary as noted in the SWD is farther south at 1502 UTC than the GFS placed it (Fig. 2a). The maximization along the line in the SWD is caused by a local deepening of water vapor due to surface convergence (Lindsey et al. 2014). Forecasters viewing the morning animations of *GOES-16* 0.64- μm visible satellite imagery and SWD would be able to find the boundary in the SWD field before any clouds have formed.

The remaining times in animations 1 and 2 and Figs. 3c and 3d show that clouds eventually do form along the east–west boundary in western Kansas, and at approximately 1812 UTC convective initiation (CI) occurs in west-central Kansas, followed by a few other CI events farther west. The initial storm goes on to produce severe weather, and the entire system later grows upscale into a mesoscale convective system, producing widespread severe wind and large hail in central and southern Kansas.

SUMMARY. On 15 June 2017, clear skies in western Kansas allowed the effective use of the *GOES-16* ABI split window difference to identify a surface boundary before any clouds had formed on the corresponding visible satellite imagery. In this case, the boundary was evident in the SWD field approximately 2 h 25 min before the first convective clouds began to

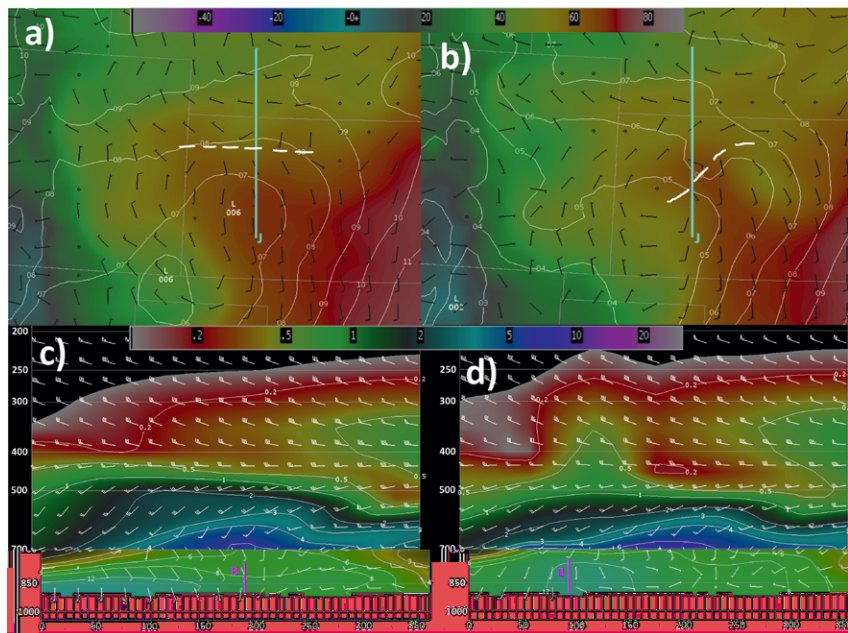


FIG. 2. GFS forecast from the 1200 UTC cycle on 15 Jun 2017, with (a),(c) the 3-h forecast valid at 1500 UTC and (b),(d) the 6-h forecast valid at 1800 UTC. Plan view of sea level pressure in hPa plotted without the leading “10” as contours and surface dewpoint in $^{\circ}\text{F}$ as the image in (a) and (b). White dashed lines are approximate locations of a surface boundary as discussed in the text. Cross sections across the cyan line in (a) and (b) are plotted in (c) and (d), with point J corresponding to 0 on the x axis of (c) and (d) and the units of the x axis being km north of point J. Both contours and the images in (c) and (d) are water vapor mixing ratio in g kg^{-1} , and the vertical axes are pressure in hPa. Yellow lines marked B are the approximate locations of the surface boundary as described in the text. The center of the domain in the plan view is western Kansas.

form along the boundary. Convergence along the boundary causes a local deepening of water vapor, and the SWD allows identification of this linear feature owing to differential absorption of water vapor between the 10.3- and 12.3- μm bands.

In practice, operational weather forecasters may be able to occasionally make use of this technique to locate low-level boundaries. Certain conditions are required: 1) clear skies in the absence of significant aerosol concentrations such as smoke or dust, 2) temperature decreasing with height in a region of locally larger water vapor content, and 3) sufficient surface convergence to produce a local pooling of low-level water vapor. These conditions came together on 15 June 2017, but on more days than not, at least one of these conditions is not met. Therefore, forecasters may check for these conditions on days with potential convective cloud formation, and occasionally the SWD technique made possible by *GOES-16*'s ABI can aid in nowcasting and short-term forecasts.

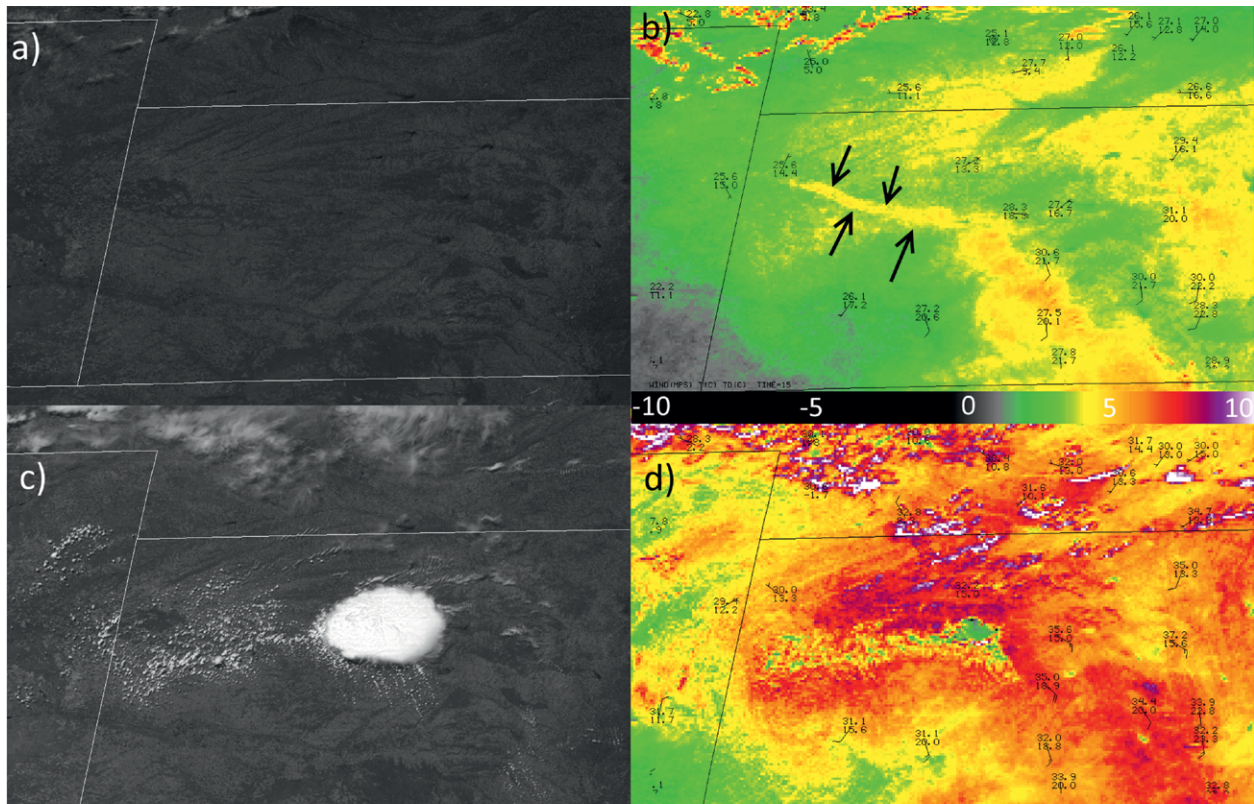


FIG. 3. (a),(c) GOES-16 0.64- μm band-2 visible images and (b),(d) the 10.3–12.3- μm SWD, valid at (a),(b) 1502 and (c),(d) 1902 UTC 15 Jun 2017. The domain is western Kansas. SWD is in units of $^{\circ}\text{C}$ of brightness temperature. Surface stations are plotted on the right column with (top) temperature and (bottom) dewpoint in $^{\circ}\text{C}$, and the wind barsbs using the convention of a full barb representing 10 m s^{-1} . Black arrows point to a feature discussed in the text. See animations 1 and 2 in the online supplement (<https://doi.org/10.1175/BAMS-D-17-0141.2>). The legend for SWD shown in (b) and (d) also applies to animation 2.

ACKNOWLEDGMENTS. This material is based on work supported by the National Oceanic and Atmospheric Administration under Grant NA14OAR4320125, as well as by the GOES-R Risk Reduction program. GOES-16 imagery shown in this paper was still preliminary and nonoperational at the time. The views, opinions, and findings in this report are those of the authors and should not be construed as an official NOAA and/or U.S. government position, policy, or decision.

FOR FURTHER READING

Chesters, D., L. W. Uccellini, and W. D. Robinson, 1983: Low-level water vapor fields from the VISSR Atmospheric Sounder (VAS) “split window” channels. *J. Climate Appl. Meteor.*, **22**, 725–743, [https://doi.org/10.1175/1520-0450\(1983\)022<0725:LLWVF>2.0.CO;2](https://doi.org/10.1175/1520-0450(1983)022<0725:LLWVF>2.0.CO;2).

Lindsey, D. T., T. J. Schmit, W. M. MacKenzie Jr., C. P. Jewett, M. M. Gunshor, and L. Grasso, 2012: 10.35

μm : Atmospheric window on the GOES-R Advanced Baseline Imager with less moisture attenuation. *J. Appl. Remote Sens.*, **6**, 063598, <https://doi.org/10.1117/1.JRS.6.063598>.

—, L. D. Grasso, J. F. Dostalek, and J. Kerkmann, 2014: Use of the GOES-R split window difference to diagnose deepening low-level water vapor. *J. Appl. Meteor. Climatol.*, **53**, 2005–2016, <https://doi.org/10.1175/JAMC-D-14-0010.1>.

Purdum, J. F. W., 1976: Some uses of high-resolution GOES imagery in the mesoscale forecasting of convection and its behavior. *Mon. Wea. Rev.*, **104**, 1474–1483, [https://doi.org/10.1175/1520-0493\(1976\)104<1474:SUOHRG>2.0.CO;2](https://doi.org/10.1175/1520-0493(1976)104<1474:SUOHRG>2.0.CO;2).

Schmit, T. J., P. Griffith, M. M. Gunshor, J. M. Daniels, S. J. Goodman, and W. J. Lebar, 2017: A closer look at the ABI on the GOES-R series. *Bull. Amer. Meteor. Soc.*, **98**, 681–698, <https://doi.org/10.1175/BAMS-D-15-00230.1>.